Research Square

Preprints are preliminary reports that have not undergone peer review.
They should not be considered conclusive, used to inform clinical practice,
or referenced by the media as validated information.

# Double-stranded RNA impairs epithelial barrier formation by redirecting airway basal cell differentiation

**Shinichi Okamoto**
Nihon University
**Shuichiro Maruoka**
Nihon University
**Kota Tsuya**
Nihon University
**Mari Hikichi**
Nihon University
**Shiho Yamada**
Nihon University
**Yusuke Kurosawa**
Nihon University
**Yutaka Kozu**
kozu.yutaka@nihon-u.ac.jp
Nihon University
**Yasuhiro Gon**
Nihon University

**Research Article**

**Keywords:** Double-stranded RNA, Poly I:C, Airway epithelial cell, Basal cell, Tight junction, Toll-like receptor 3, Air liquid interface

**Posted Date:** September 10th, 2026

**DOI:** https://doi.org/10.21203/rs.3.rs-10722690/v1

**License:** This work is licensed under a Creative Commons Attribution 4.0 International License.
Read Full License

**Additional Declarations:** No competing interests reported.

**Version of Record:** A version of this preprint was published at BMC Molecular and Cell Biology on November 4th, 2026. See the published version at https://doi.org/10.1186/s12860-026-00610-x.

## Abstract

# Background

Viral double-stranded RNA disrupts the airway epithelial barrier, but its specific impact on progenitor basal cells remains unknown. In this study, we stimulated undifferentiated normal human bronchial epithelial cells and VA10 cells, which function as basal cells, with the Toll-like receptor 3 (TLR3) ligand polycytidylic acid (poly I:C). The cells were subsequently cultured at an air-liquid interface (ALI) to evaluate airway epithelial barrier integrity and perform global gene expression analysis.

# Results

Poly I:C stimulation significantly decreased trans-epithelial electrical resistance and reduced the expression of barrier-related genes. This barrier dysfunction was improved by silencing TLR3 or TIR-domain-containing adapter-inducing interferon-β. Transcriptomic analysis revealed a biphasic response to poly I:C. During the late phase, the transcriptional landscape shifted toward sustained inflammation and abnormal tissue remodeling. During the early phase, the transcriptomic profile suggests the initial prioritization of an antiviral state, which may affect essential epithelial differentiation and barrier genes.

# Conclusions

Exposure of airway basal cells to double-stranded RNA triggered a TLR3/ TIR-domain-containing adapter-inducing interferon β-mediated biphasic response. An initial prioritization of antiviral defence compromises epithelial differentiation, which is followed by a late phase of unresolved chronic inflammation and abnormal remodeling. This cascade may provide a potential mechanistic explanation for how viral infections induce persistent airway barrier vulnerability and chronic dysfunction.

## Background

Bronchial asthma is a chronic inflammatory disease of the airways characterized by coughing, wheezing, variable airflow limitation, and airway hyperresponsiveness. The pathogenesis of asthma is related to genetic and environmental factors such as allergens, smoking, and viral infections [1]. Viral infections such as those caused by rhinoviruses, which are major exacerbating factors of asthma, induce damage to airway epithelial cells and disrupt barrier function [2–4]. Previous studies have suggested that viral infections induce subsequent asthma onset. Pattern recognition receptors such as Toll-like receptors (TLRs), which are present in airway epithelial cells and macrophages, recognize conserved molecular structures such as pathogen-associated molecular patterns. These are components of pathogenic microorganisms, including viruses and bacteria, and elicit immune response [5–7]. TLR4 is activated by bacterial membrane and mite allergens (lipopolysaccharide: LPS). TLR5 is activated by bacterial flagellar component proteins (flagellin), whereas TLR9 is activated by CpG DNA, which is bacterial DNA. TLR3 is

activated by double-stranded RNAs (dsRNAs), which are synthesized during the intermediate replication stage of viral infection and induce airway inflammation [8,9]. Viral infection of epithelial cells has been reported to promote the production of type I interferons (IFNs) through TLR3 [10,11], and dsRNAs are involved in disrupting airway epithelial barrier function [12–16].

The airway epithelium comprises goblet, ciliated, and club cells on the luminal side and basal cells on the basement membrane. Airway epithelial cells have intercellular barrier junctions, such as tight junctions (TJ) and adherens junctions. TJs are formed by the intercellular binding of transmembrane proteins, such as members of the claudin family, occludin, zonula occludens (ZO) 1–3, and junctional adhesion molecule (JAM)-1 [17–19]. In addition to mucus production by goblet cells and clearance of airways by ciliated cells, this epithelial barrier is important for preventing the entry of environmental factors, such as allergens, house dust, and viruses into the body [20]. It has been reported that the airway epithelial barrier in patients with asthma is more vulnerable than that in healthy individuals. This is because the airway epithelium is disrupted and can be easily infiltrated by environmental factors, leading to allergic airway inflammation [20]. A previous study demonstrated that steroids enhance airway epithelial barrier function [21], and dsRNAs reduce the expression of TJ molecules [15] and target molecules involved in enhancing airway epithelial barrier integrity [22,23]. Thus, the airway epithelial barrier function is important in the pathogenesis of asthma and enhancing or suppressing its disruption may lead to new treatments for asthma. As described above, viral infections in childhood induce subsequent asthma development, and the epithelial barrier function is decreased by TLR3, a viral defense mechanism. Viral infection may affect the early stages of epithelial barrier formation, leading to vulnerability of epithelial barrier integrity in patients with asthma.

In addition to their self-renewal capacity, basal cells can differentiate into goblet and ciliated cells and are involved in the repair of damage to the airway epithelium. Basal cells are characterized by the overexpression of cytokeratin (CK) 5,14 and transcription factor p63 [24]. Persson et al. reported that viral infection of basal cells induces goblet cell hyperplasia [25]. However, the mechanism by which the viral infection of basal cells affects subsequent formation of the epithelial barrier is not fully understood. Thus, we focused on airway basal cells and investigated the mechanism underlying the early stages of epithelial barrier formation, which leads to the disruption of the epithelial barrier by dsRNAs.

## Methods

# Cells and reagents

Normal human bronchial epithelial cells (NHBECs) were purchased from Lonza Walkersville, Inc. (Basel, Switzerland). VA10 cells, a human airway basal cell line, was donated by Dr. Shuichi Hashimoto, a professor in the Department of Anatomy and Anthropology, Division of Basic Medical and Dental Sciences, Fukuoka Dental University, with permission from Dr. Thorarinn Gudjonsson of Landsat University Hospital. VA10 cells are NHBECs immortalized by transfecting the HPV16-derived E6/E7

oncogene using a retrovirus. Poly I:C and flagellin were purchased from InvivoGen (San Diego, CA). LPS and CpGB DNA were purchased from Sigma-Aldrich (St. Louis, MO, USA) and HyCult Biotech (PB, Uden, Netherlands), respectively. Fluorescein isothiocyanate-labeled dextran ( 10 kDa) was purchased from Sigma-Aldrich (St. Louis, MO, USA).

## Cell culture

NHBECs were cultured in PneumaCult$^{TM}$-Ex Medium (STEMCELL Technologies, Vancouver, Canada), and VA10 cells were cultured in LHC-9 medium (Thermo Fisher Scientific, Tokyo, Japan) in a humidified 5% $CO_2$ and 37°C incubator. NHBECs and VA10 cells were submerged in liquid-covered culture (LCC) medium for 3 days in collagen-treated transwell chambers (Costar, Washington DC, USA), and the upper transwell culture medium was removed to induce cell differentiation. The lower layer of the culture medium was replaced with PneumaCult$^{TM}$-ALI Medium (STEMCELL Technologies) for NHBECs and Dulbecco's Modified Eagle's Medium (DMEM) and Ham's F-12 Nutrient 1:1 Mixture (DMEM/F-12) (Thermo Fisher Scientific) containing Ultrocer$^{TM}$G (Pall Corporation, Port Washington, NY, USA) for VA10; culture was continued for 7 days (air-liquid interface: ALI). The cells were cultured with poly I:C (TLR3 ligand, 10 μg/ml), LPS (TLR4 ligand, 10μg /ml), flagellin (TLR5 ligand,1μg /ml), or CpG-DNA (TLR9 ligand, 5μM), in LCCs for 3 days and incubated in ALI culture with medium alone until day 10.

## Transepithelial electrical resistance measurements

To evaluate the epithelial barrier function after ALI culture, the transepithelial electrical resistance (TEER) between the cell layers was measured by passing current through the electrodes in the upper and lower Transwell layers. We evaluated the formation and changes in the barrier between the cell layers by measuring the electrical resistance between them. TEER values were measured using Millicell®-ERS (Millipore, Billerica, MA, USA) and corrected by subtracting the baseline values measured in inserts without the cells and with only the media in both chambers. The final values were calculated as the difference between TEER sample and TER blank values given in TER units $\Omega \times cm^2$. Measurements were taken up to day 10, with the ALI start date of day 3.

## Apparent permeability coefficient (Papp)

The permeability of the cell monolayer was determined using a fluorescein isothiocyanate-dextran flux (FITC-dextran) across this layer. A solution containing 10-kDa FITC-dextran (1 mg/mL) was added to the apical compartment of the Transwell insert. Samples (200 μL) were removed from the basal compartments at 60 min after the addition of FITC-dextran. FITC-dextran intensity was measured using a PTI fluorometer at an excitation wavelength of 492 nm and an emission wavelength of 520 nm. Papp was obtained using the following equation:

$$Papp\ (cm/s) = \frac{Q}{dt}(V/A\ C0)$$

where Q/dt is the permeability rate (g/s), C0 is the initial concentration in the upper chamber (g/mL), V is the volume of the upper chamber ($cm^3$), and A is the membrane surface area ($cm^2$) [21].

## Fluorescence immunostaining

NHBECs under LCC were attached to glass slides by cytospin using an AutoAmear centrifuge (Sakura Finetek, Torrance, CA, USA), fixed with 4% paraformaldehyde, and stained as previously described. The cells were stained with monoclonal mouse anti-CK5 (GeneTex, Irvine, CA, USA) and monoclonal mouse anti-CK14 (Abcam, Cambridge, UK) primary antibodies, followed by secondary antibody staining with anti-mouse IgG Alexa 488 (Invitrogen, Carlsbad, CA, USA). Images were captured using a fluorescence microscope (BZ-X700; Keyence, Osaka, Japan).

# Small interfering RNA preparation and transfection

To investigate whether poly I:C stimulation of basal cells is involved in barrier depletion via the TLR3 and TIR-domain-containing adapter-inducing IFNβ (TRIF) pathways, we performed experiments using specific short interfering RNAs (siRNAs). TLR3- and TRIF-specific siRNAs (5 nM) were transfected into VA10 cells using Lipofectamine™ RNAiMAX (Thermo Fisher Scientific) according to the manufacturer's protocol. Transfected cells were trypsinized, transferred to a transwell chamber for 24 h, stimulated with poly I:C, and cultured in ALI as described above. The effect on barrier function was examined by measuring the TEER. The following siRNAs were used for transfection: Stealth RNAi™ siRNA Negative Control Med GC Duplex #2 (Invitrogen); TLR3 siRNA (Invitrogen); TLR3_HSS110816 (3 RNAi) HUMAN NM_003265; TICAM1 (TRIF) siRNA (Sigma); and SASI_Hs01_00226929 HUMAN NM_014261.

## Real-time quantitative PCR

Real-time quantitative polymerase chain reaction (PCR) (RT-qPCR) was performed using the Ambion TaqMan Green Cells-to-CT kit (Thermo Fisher Scientific) and Ambion Fast SYBR Green Cells-to-CT kit (Life Technologies, Carlsbad, CA, USA), according to the manufacturer's protocols. After sample preparation, PCR was performed using an Applied Biosystems StepOnePlus Real-Time PCR System (Foster City, CA, USA). We set the initial threshold and determined the Ct values. We evaluated the gene expression levels of each sample using the comparative determination method (ΔΔCT method). The primers used for TaqMan were as follows: Keratin 5: Hs00361185_m1; Keratin 14: Hs00265033_m1; FLG (filaggrin): Hs00856927_g1

IFI27: Hs01086373_g1; IFI6:Hs00242571_m1; KRT10:Hs00166289_m1; DSG1:Hs00355084_m1.

The primer sequences for SYBR are shown in Table 1.

Table 1
Specific primers for real-time polymerase chain reaction.

| Primers | Forward 5'→3' | Reverse 5'→3' |
|---|---|---|
| E-cadherin | AAGGTGACAGAGCCTCTGGATAGA | CATTCCCGTTGGATGACACA |
| Occludin | CGAGGAGTGGGTTAAAAATGTGT | ACTGTCAACTCTTTCCACATAGTCAGA |
| ZO-1 | CGGTCCTCTGAGCCTGTAAG | GGATCTACATGCGACGACAA |
| ZO-2 | GAGGAGTAGGAGCAGGAGCA | GGAGCCAACCTGACAGCTC |
| JAM-A | CCGTGTGGAGTGGAAGTTTGA | TCACCCGGTCCTCATAGGAA |
| JAM-B | GCCTGCAAAACCCCAAAGAA | GAGACACTCCGACCCAGTTT |
| JAM-C | TCAGCCCTTTATCGCTGTGA | GTACAGCCTTCGGCACTCTA |
| CLDN 1 | GGATTTACTCCTATGCCGGCGACAACA | CTCTGCGACACGCAGGACATCCA |
| CLDN 3 | CATCACGTCGCAGAACATCTG | TCGTACACCTTGCACTGCATCT |
| CLDN 4 | AGCCTTCCAGGTCCTCAACT | AGCAGCGAGTCGTACACCTT |
| CLDN 5 | CCTGGACCACAACATCGTGA | AGCACCGAGTCGTACACTTT |
| CLDN 6 | ATGCAGTGCAAGGTGTACGA | CCAGCAAGGTAGACCAGCAA |
| CLDN 7 | AGGCATAATTTTCATCGTGG | GAGTTGGACTTAGGGTAAGAGCG |
| CLDN 9 | ATGCAGTGCAAGGTGTACGA | TACACTGGGCACCTGTGATG |
| CLDN 11 | CCCGGTGTGGCTAAGTACAG | GATTGTGGGAGTCCATCCCC |
| CLDN 16 | TGGGAATGCGTCACAAATGC | GGATGCTCCGCAAGTATGGA |
| CLDN 18 | TACACATTTGGTGCGGCTCT | TAAAACGTCTGGTTGCAGCG |
| CLDN 19 | GCATTGACAGGTGTGCTTGG | CAGCCCGACTCAGTGTCATC |
| TAGLN | GGCCAAGGCTCTACTGTCTG | CCCTTGTTGGCCATGTCT |
| IL-6 | TGTAGCCGCCCCACACA | CCGTCGAGGATGTACCGAAT |
| CXCL8(IL-8) | GCTGGCCGTGGCTCTCT | TTAGCACTCCTTGGCAAAACTG |
| TNFAIP3 | CTGCCCAGGAATGCTACAGATAC | GTGGAACAGCTCGGATTTCAG |
| TLR3 | ATTGGCCTCTTTCTGAACAAT | ATTCCGAATGCTTGTGTTTGC |
| TRIF | AAGGTGGCCAACACCTTCAA | TGAGTAGGCTGCGTTCAGTG |

[Insert Table 1 here]

# Microarray analysis

NHBECs were cultured in LCC and divided into control and polyI:C-stimulated groups, as described above. Total RNA was extracted from the cells using the QIAGEN RNeasy Mini Kit (QIAGEN, Valencia, CA, USA) on days 3 and 10 of culture. RNA integrity was confirmed using the Agilent RNA 6000 Nano Kit (Agilent Technologies, Palo Alto, CA). The Clariom S Assay (Thermo Fisher Scientific) was used to synthesize cDNA and cRNA from total RNA according to the manufacturer's protocol, and the fragmented DNA was labeled. The arrays were hybridized, washed, and stained using GeneChip Fluidics Station 450 and scanned with GeneChip Scanner 3000 (Affymetrix) to measure fluorescence intensity.

For the Day 10 time point, independent biological replicates (n = 4 per group) were analyzed to evaluate statistical significance. The gene expression data obtained were subjected to statistical analysis using the Transcriptome Analysis Console (Thermo Fisher Scientific) to identify genes whose expression varied significantly upon polyI:C stimulation. P-values were adjusted for multiple testing using the Benjamini–Hochberg False Discovery Rate (FDR) method. Differentially expressed genes (DEGs) on day 10 were identified based on both statistical significance (FDR < 0.05) and magnitude of change (fold change > 2.0 or < 0.5), and the results were visualized using a volcano plot.

Due to the limited amount of RNA obtained from individual wells on day 3, equal amounts of RNA from three independent wells were pooled into a single sample per group (n = 1). DEGs on day 3 were defined using an exploratory approach based on a fold-change cutoff of > 2.0 or < 0.5, and the global expression profile was visualized using a scatter plot.

# Statistical analysis

Data are presented as mean ± standard deviation (SD). Differences between experimental groups were analyzed using an unpaired t-test or one-way analysis of variance (ANOVA), followed by Dunnett’s multiple comparison test. Statistical significance was set at $p < 0.05$. significant. All statistical analyses were performed using GraphPad Prism version 7.0 (GraphPad Software, La Jolla, CA, USA).

## Results

# Poly I:C stimulation of NHBECs during LCC induced epithelial barrier dysfunction in ALI cultures

The basal cell phenotype of the NHBECs in the liquid-covered culture (LCC) was confirmed by positive staining for CK5 and CK14 (Supplement 1).

The experiment was conducted over time as shown in Fig. 1a. We investigated the effects of TLR3, 4, 5, and 9 ligands on the early stages and subsequent steps of epithelial barrier formation and subsequent steps. NHBECs composed of basal cells were cultured in submerged medium (LCC) in a Transwell plate for 3 days, with or without ligands. The cells were subsequently exposed to ALI without ligands for 7

days. TEER significantly decreased in cells treated with poly I:C, a TLR3 ligand, compared to that in untreated cells (Fig. 1b).

**Poly I:C stimulation of VA10 cells** dur**in**g **LCC-induced epithelial barrier dysfunction in ALI cultures**

The experiment was conducted over the time course shown in Fig. 2a.

To examine the effect of poly I:C on basal cells, we performed experiments using VA10 cells, the basal cell line. To verify barrier disruption by poly I:C, we performed the same experiments as those for NHBECs. TEER was significantly decreased on day 10 in cells treated with poly I:C relative to that in untreated cells (Fig. 2b). We also observed a significant increase in the FITC-dextran permeability in the poly I:C-treated group (Fig. 2c). On day 10, barrier-related gene expression was confirmed using real-time PCR. The expression levels of claudin-3, -9, and-11, ZO-2, and JAM-C decreased significantly (Fig. 2d).

**Epithelial barrier dysfunction via TLR3 pathway in basal cells**

These results suggested that poly I:C affects epithelial barrier formation in VA10 cells. To identify the signaling pathways involved in this process, we investigated whether poly I:C stimulation in basal cells impaired the barrier *via* the TLR3 and TRIF pathways using specific siRNAs. First, using RT-qPCR, we confirmed a significant reduction in TLR3 and TRIF mRNA expressions in VA10 cells after siRNA transfection (Supplement 2). In ALI cultures, poly I:C treatment significantly suppressed the reduction in TEER on day 10 in cells in which TLR3 and TRIF genes were silenced relative to that in cells transfected with control siRNAs (Fig. 2e).

# Microarray analysis (day 10)

Microarray analysis was performed on day 10 after the polyI:C stimulation of basal cells to investigate whether there were any changes in gene expression, as this stimulation was involved in barrier impairment. Total RNA was extracted from NHBECs on day 10 of ALI in the polyI:C-stimulated (n = 4) and non-stimulated (n = 4) LCC groups, and gene analysis was performed using DNA microarrays. Among the 21448 genes implemented in the microarray, we identified 159 genes that were significantly ($p < 0.05$) upregulated or downregulated 2-fold. The number of upregulated and downregulated genes was 80 and 79, respectively. The top 10 genes among the upregulated genes are mapped (Fig. 3a). Among the upregulated genes, we identified pro-inflammatory cytokines, such as IL-1A, IL-1B, IL-6, and CXCL8(IL-8), and TNFAIP3, which is known to play an anti-inflammatory role. Furthermore, genes associated with tissue remodeling and cytoskeletal reorganization, including ADAM9 and TAGLN, were significantly induced. Conversely, genes enriched in club and secretory cells, such as ALDH3A1 and BPIFB1, were downregulated.

The most significantly upregulated and downregulated genes were selected and validated using real-time PCR. The expression of genes related to inflammatory cytokines (IL8, IL-6, and TNFAIP3)and the remodeling-related gene TAGLN was significantly increased (Fig. 3b).

# Microarray analysis (day 3)

To examine what was happening in the cells immediately before basal cell differentiation, we performed microarray analysis on day 3 after poly I:C stimulation. Total RNA was extracted from NHBECs on day 3 of LCC in the poly I:C-stimulated and non-stimulated groups of LCC, and gene analysis was performed using DNA microarrays. Microarray analysis was performed by pooling the three samples. Among the 21448 genes implemented in the microarray, we identified 1679 genes whose fold change was upregulated or downregulated 2-fold. The numbers of upregulated and downregulated genes were 859 and 820, respectively. The top 10 upregulated and downregulated genes were mapped (Fig. 4a). Several upregulated genes, including IFN-related genes, were identified. Additionally, we observed a significant downregulation of genes involved in epithelial differentiation and barrier formation, such as FLG (filaggrin), Desmoglein-1 (DSG1), and keratin 10 (KRT10).

Among the genes identified via microarray analysis on day 3, the most significantly upregulated and downregulated were selected and validated using real-time PCR. In the stimulated group, we observed upregulation of IFN-related genes (IFI27 and IFI6) and downregulation of barrier-associated genes (FLG, KRT10, and DSG1) on day 3 (Fig. 4b).

# Effects of type I IFN stimulation of basal cells on airway barrier function

Based on the above microarray results, many of the top 10 genes were associated with IFN. Poly I:C stimulates the production of type I IFNs and pro-inflammatory cytokines via the TLR3/TRIF pathway. Type I IFNs attenuate the barrier of the gastrointestinal epithelium. Therefore, we determined whether type I IFNs were directly involved in epithelial barrier impairment. IFNα and IFNβ treatments (10, 100, 500 U/mL) were applied to VA10 cells in LCC for only 3 days, and TEER was measured over time under ALI. No significant change was observed in the TEER for up to day 10 of ALI for the stimulated group relative to that for the non-stimulated group (Fig. 4c). Under the present experimental conditions, type I IFN stimulation alone did not reproduce the barrier impairment induced by poly I:C in basal cells.

## Discussion

This study revealed that stimulating airway basal cells with poly I:C (dsRNA) induces a profound and lasting impairment of epithelial barrier function via the TLR3/TRIF pathway. Viral infections are a primary environmental factor in the pathogenesis and exacerbation of asthma and are known to compromise airway epithelial integrity. Previous reports have established that poly I:C can disrupt the barrier of differentiated epithelia, but its impact on the regenerative and maturational capacities of basal cells remains unclear.

To understand the specific effects of poly I:C, we first examined how various pathogen-associated molecular pattern ligands affect basal cell stimulation and subsequent barrier function. We confirmed

that stimulating basal cells with poly I:C (a TLR3 ligand) significantly impaired subsequent epithelial barrier formation. In contrast, stimulation with a TLR9 ligand (CpG-DNA) enhanced barrier formation, which is consistent with previous reports [15,26]. This initial screening underscored the potent and specific detrimental effects of TLR3 activation on epithelial regeneration, prompting a deeper investigation of its mechanism.

Our results further demonstrate that the observed barrier dysfunction depends on the canonical innate immune sensors for dsRNA TLR3 and its adaptor protein TRIF. This pathway activates transcription factors, such as IRF3 and NF-κB, that orchestrate antiviral and inflammatory responses, respectively [10,11,27]. These results extend those of previous studies showing that poly I:C stimulation reduces airway epithelial barrier function via TLR3 signaling. In the present study, the transcriptional levels of classical junctional molecules, such as E-cadherin and occludin, were not reduced. As previously reported, epithelial barrier integrity is likely influenced not only by protein abundance but also by the spatial localization of junctional proteins and compositional changes within the claudin family [15,21,26,28,29].

To elucidate the underlying molecular pathogenesis, we performed microarray analysis, which revealed a distinct, biphasic transcriptional program. We first characterized the late phase (day 10), when the transcriptional landscape shifted toward sustained inflammation and tissue remodeling. The expression of key pro-inflammatory cytokines, including IL-6 and CXCL8 (IL-8), remained significantly elevated. Previous studies have reported that these cytokines are induced by polyI:C stimulation via TLR3 and they affect the barrier [27,30–33]. This persistent inflammatory signaling, originating from the epithelium itself, likely perpetuates barrier defects and contributes to the chronic inflammatory environment, which is characteristic of viral exacerbations. Additionally, we observed an increased expression of genes associated with airway epithelial remodeling and fibrosis, including TAGLN [34,35]. These findings suggest that prolonged inflammatory stress drives abnormal structural alterations, potentially predisposing the airway to pathological remodeling. Taken together, these transcriptomic shifts may increase the susceptibility of the airway epithelium to further injury, perpetuating a vicious cycle of impaired repair, chronic inflammation, and airway remodeling.

To understand how this late-phase phenotype was established, we investigated the early phase cellular responses just before basal cell differentiation (day 3). This early phase was characterized by an antiviral state marked by the significant induction of several interferon-stimulated genes (ISGs), such as IFI6, RSAD2 (viperin), IFI27, and IFI44L. The genes, which have been reported to be upregulated during influenza and SARS-CoV-2 infections, were identified as hub genes that exert central regulatory control over broader gene networks [36–38]. Type I IFN induces ISG expression However, direct stimulation with type I interferons (IFN-α and IFN-β) did not replicate the barrier defect in our model (Fig. 4c). This suggests that the impairment of barrier function is likely caused by other downstream effector factors although an IFN response is induced.

Concurrently, we observed a significant downregulation of genes essential for epithelial differentiation and barrier integrity, including FLG, DSG1, and KRT10. Filaggrin (FLG) is a structural protein essential for

epithelial barrier formation and maintenance. Originally identified in the stratum corneum of the skin, FLG aggregates keratin filaments and facilitate the terminal differentiation of keratinocytes and establish a physical defense against exogenous allergens and pathogens [39]. Recent evidence has demonstrated constitutive FLG expression in the human respiratory mucosa, specifically in ciliated and basal cells of the nasal and bronchial epithelia [39,40]. FLG deficiency is a well-established risk factor for atopic dermatitis and is strongly associated with early onset and severe asthma. In the airway epithelium, reduced FLG increases paracellular permeability and triggers the release of pro-inflammatory cytokines such as Thymic Stromal Lymphopoietin (TSLP) and IL-33, which exacerbate Th2-mediated allergic inflammation. Furthermore, elevated IL-4 concentrations downregulated FLG expression in respiratory epithelial cells [41–43].

DSG1 is a transmembrane glycoprotein that belongs to the cadherin superfamily and is a critical component of desmosomes. They provide mechanical strength and structural integrity by mediating cell-to-cell adhesion. DSG1 has traditionally been recognized for its role in the skin; however, recent studies have highlighted its presence and functional importance in the respiratory tract. DSG1 is expressed throughout the human airway epithelium, including the bronchial mucosa, where it is a critical component of the desmosomes that maintain structural cohesion [44]. The clinical relevance of DSG1 in airway diseases has been demonstrated in asthma models. DSG1 expression was significantly reduced in the bronchial epithelium during asthma recurrence induced by house dust mites (HDM) [44]. Similar to the skin and esophagus, reduced DSG1 expression in the airways leads to impaired barrier integrity, which is characterized by decreased TEER and increased paracellular flux [45,46]. Further, DSG1 regulates epithelial immune responses in the airways. DSG1 deficiency has been associated with Thymic Stromal Lymphopoietin (TSLP) upregulation [44]. Together, these observations suggest that the loss of DSG1 in the airway epithelium compromises the physical barrier and promotes an environment conducive to allergic sensitization and chronic airway inflammation. Therefore, DSG1 plays a pivotal role in the pathogenesis and recurrence of asthma.

Finally, the expression of KRT10, a type I intermediate filament protein, was evaluated. Although typically absent from healthy, pseudostratified airway epithelium, KRT10 is induced under conditions of chronic inflammation or injury, which is a hallmark of squamous metaplasia [47–49]. However, KRT10 was significantly downregulated alongside the essential structural proteins FLG and DSG1. Instead of indicating a protective effect against pathological remodeling, the concurrent suppression of both normal and aberrant differentiation markers suggests an arrest in the differentiation trajectory.

Our findings are consistent with the evidence linking viral infection of basal cells to impaired epithelial repair. For instance, inflammatory signals present in severe cases of COVID-19 have been reported to hinder the differentiation of basal cells into ciliated cells while promoting goblet cell hyperplasia. Similarly, basal cell infection by respiratory syncytial virus (RSV) induces interferon production and promotes differentiation into mucus-producing cells [25,50].

Collectively, these early transcriptional profiles suggest that airway basal cells prioritize immediate antiviral defenses at the expense of structural maturation upon viral sensing. As the primary stem cells of the respiratory epithelium, basal cells dictate the trajectory of tissue repair [51]. Unlike terminally differentiated epithelial cells, they mount a robust innate immune response that can leave a lasting inflammatory imprint on the regenerating tissue [50]. Our data demonstrate that exposure to dsRNA during the critical early window of differentiation activates a potent antiviral program that completely disrupts the normal structural assembly. These findings suggested that early viral infections lead to barrier dysfunction and chronic inflammation.

This study has limitations. First, we used poly I:C as a viral mimic, but this does not capture the full complexity of a live viral infection. Further studies using viral models are required to validate our findings. Second, our study focused on transcriptional changes. Further research is required to confirm these alterations at the protein level, including the expression and localization of other barrier-related proteins. Additionally, it is necessary to assess the functional consequences, such as changes in mucus production and ciliary motility.

## Conclusion

In summary, our findings demonstrated that a single poly I:C challenge in airway basal cells triggered a two-phase response that resulted in persistent epithelial pathology. Early prioritization of antiviral defense compromises the fundamental program of epithelial differentiation. This transition leads to a late phase of inflammation and abnormal remodeling, resulting in the failure of epithelial maturation. This cascade is orchestrated via the TLR3/TRIF pathway. Our results suggest that the viral infection of airway basal cells is pivotal to the pathogenesis of chronic airway inflammation. It occurs not only through acute damage but also by inducing long-term dysregulation of epithelial regeneration and chronic barrier dysfunction.

## Abbreviations

| | |
|---|---|
| ALI | Air-liquid interface |
| dsRNA | double-stranded RNA |
| FITC-dextran | Fluorescein isothiocyanate-dextran flux |
| NHBECs | Normal human bronchial epithelial cells |
| poly I:C | polyinosinic polycytidylic acid |
| RS viruses | Respiratory syncytial viruses |
| RT-qPCR | Real-time quantitative PCR |

| | |
|---|---|
| SD | Standard deviation |
| siRNAs | Short interfering RNAs |
| TEER | Trans-epithelial electrical resistance |
| TLR 3 | Toll-like receptor 3 |
| TRIF | TIR-domain-containing adapter-inducing interferon-β |

## Declarations

**Ethics approval and consent to participate**

Not applicable

**Consent for publication**

Not applicable

# Competing interests

The authors declare no competing interests.

# Funding

This work was supported by the following grants: a Grant-in-Aid for Scientific Research (C) (18K07482) from the Ministry of Education, Culture, Sports, Science, and Technology (MEXT), The Strategic Research Base Development Program for Private Universities subsidized by MEXT (S1511014) a Nihon University Multidisciplinary Research Grant for 2021, and a research grant from Nihon University.

# Author Contribution

SO and SM designed the study and prepared initial drafts of the manuscript. KT, MH, SY, YKo, and YKu conceived and planned the experiments. YG contributed to data analysis and interpretation and assisted in the preparation of the manuscript. All authors contributed to the interpretation of data and critically reviewed the manuscript.

# Acknowledgement

We thank Ms. Ikuko Takeshita and Ms. Kaori Soda (Division of Respiratory Medicine, Department of Internal Medicine, Nihon University School of Medicine, Tokyo, Japan) for technical assistance. Funding: This study was supported by the Department of Microbiology and Immunology, Division of Immunology and Pathobiology, Dental Research Center, Nihon University School of Dentistry, Japan.We would like to thank Editage (www.editage.jp) for English language editing.

# Data Availability

The datasets generated during and/or analyzed during the current study are available from the corresponding author upon reasonable request

## References

1. Wenzel SE. Asthma phenotypes: the evolution from clinical to molecular approaches. Nat Med. 2012;18:716–25.
2. Comstock AT, Ganesan S, Chattoraj A, et al. Rhinovirus-induced barrier dysfunction in polarized airway epithelial cells is mediated by NADPH oxidase 1. J Virol. 2011;85:6795–808.
3. Sajjan U, Wang Q, Zhao Y, Gruenert DC, Hershenson MB. Rhinovirus disrupts the barrier function of polarized airway epithelial cells. Am J Respir Crit Care Med. 2008;178:1271–81.
4. Jackson DJ, Gangnon RE, Evans MD, et al. Wheezing rhinovirus illnesses in early life predict asthma development in high-risk children. Am J Respir Crit Care Med. 2008;178:667–72.
5. Aoshi T, Koyama S, Kobiyama K, Akira S, Ishii KJ. Innate and adaptive immune responses to viral infection and vaccination. Curr Opin Virol. 2011;1:226–32.
6. Murakami Y, Fukui R, Motoi Y, et al. Roles of the cleaved N-terminal TLR3 fragment and cell surface TLR3 in double-stranded RNA sensing. J Immunol. 2014;193:5208–17.
7. Satoh T, Akira S. Toll-Like Receptor Signaling and Its Inducible Proteins. Microbiol Spectr 2016;4.
8. Holtzman MJ, Byers DE, Alexander-Brett J, Wang X. The role of airway epithelial cells and innate immune cells in chronic respiratory disease. Nat Rev Immunol. 2014;14:686–98.
9. Lambrecht BN, Hammad H. Allergens and the airway epithelium response: gateway to allergic sensitization. J Allergy Clin Immunol. 2014;134:499–507.
10. Vercammen E, Staal J, Beyaert R. Sensing of viral infection and activation of innate immunity by toll-like receptor 3. Clin Microbiol Rev. 2008;21:13–25.
11. Uematsu S, Akira S. Toll-like receptors and Type I interferons. J Biol Chem. 2007;282:15319–23.
12. Rezaee F, Meednu N, Emo JA, et al. Polyinosinic:polycytidylic acid induces protein kinase D-dependent disassembly of apical junctions and barrier dysfunction in airway epithelial cells. J Allergy Clin Immunol. 2011;128:1216–e2411.
13. Sweerus K, Lachowicz-Scroggins M, Gordon E, et al. Claudin-18 deficiency is associated with airway epithelial barrier dysfunction and asthma. J Allergy Clin Immunol. 2017;139:72–81. e1.

14. Huang LY, Stuart C, Takeda K, D'Agnillo F, Golding B. Poly(I:C) Induces Human Lung Endothelial Barrier Dysfunction by Disrupting Tight Junction Expression of Claudin-5. PLoS ONE. 2016;11:e0160875.
15. Gon Y, Maruoka S, Kishi H et al. DsRNA disrupts airway epithelial barrier integrity through down-regulation of claudin members. Allergol Int 2016;65 Suppl:S56-8.
16. Schulz O, Diebold SS, Chen M, et al. Toll-like receptor 3 promotes cross-priming to virus-infected cells. Nature. 2005;433:887–92.
17. Stevenson BR, Siliciano JD, Mooseker MS, Goodenough DA. Identification of ZO-1: a high molecular weight polypeptide associated with the tight junction (zonula occludens) in a variety of epithelia. J Cell Biol. 1986;103:755–66.
18. Tsukita S, Yamazaki Y, Katsuno T, Tamura A, Tsukita S. Tight junction-based epithelial microenvironment and cell proliferation. Oncogene. 2008;27:6930–8.
19. Niessen CM. Tight junctions/adherens junctions: basic structure and function. J Invest Dermatol. 2007;127:2525–32.
20. Holgate ST. Epithelium dysfunction in asthma. J Allergy Clin Immunol. 2007;120:1233–44. quiz 45 – 6.
21. Sekiyama A, Gon Y, Terakado M, et al. Glucocorticoids enhance airway epithelial barrier integrity. Int Immunopharmacol. 2012;12:350–7.
22. Kozu Y, Gon Y, Maruoka S, et al. Protocadherin-1 is a glucocorticoid-responsive critical regulator of airway epithelial barrier function. BMC Pulm Med. 2015;15:80.
23. Shintani Y, Maruoka S, Gon Y, et al. Nuclear factor erythroid 2-related factor 2 (Nrf2) regulates airway epithelial barrier integrity. Allergol Int. 2015;64(Suppl):S54–63.
24. Rock JR, Hogan BL. Epithelial progenitor cells in lung development, maintenance, repair, and disease. Annu Rev Cell Dev Biol. 2011;27:493–512.
25. Persson BD, Jaffe AB, Fearns R, Danahay H. Respiratory syncytial virus can infect basal cells and alter human airway epithelial differentiation. PLoS ONE. 2014;9:e102368.
26. Kubo T, Wawrzyniak P, Morita H, et al. CpG-DNA enhances the tight junction integrity of the bronchial epithelial cell barrier. J Allergy Clin Immunol. 2015;136:1413–e61.
27. Lever AR, Park H, Mulhern TJ et al. Comprehensive evaluation of poly(I:C) induced inflammatory response in an airway epithelial model. Physiol Rep 2015;3.
28. Al-Sadi RM, Ma TY. IL-1beta causes an increase in intestinal epithelial tight junction permeability. J Immunol. 2007;178:4641–9.
29. Wittekindt OH. Tight junctions in pulmonary epithelia during lung inflammation. Pflugers Arch. 2017;469:135–47.
30. Suzuki T, Yoshinaga N, Tanabe S. Interleukin-6 (IL-6) regulates claudin-2 expression and tight junction permeability in intestinal epithelium. J Biol Chem. 2011;286:31263–71.

31. Willart MA, Deswarte K, Pouliot P, et al. Interleukin-1alpha controls allergic sensitization to inhaled house dust mite via the epithelial release of GM-CSF and IL-33. J Exp Med. 2012;209:1505–17.
32. Coyne CB, Vanhook MK, Gambling TM, Carson JL, Boucher RC, Johnson LG. Regulation of airway tight junctions by proinflammatory cytokines. Mol Biol Cell. 2002;13:3218–34.
33. Leino MS, Loxham M, Blume C, et al. Barrier disrupting effects of alternaria alternata extract on bronchial epithelium from asthmatic donors. PLoS ONE. 2013;8:e71278.
34. Fehrholz M, Speer CP, Kunzmann S. Caffeine and rolipram affect Smad signalling and TGF-beta1 stimulated CTGF and transgelin expression in lung epithelial cells. PLoS ONE. 2014;9:e97357.
35. Kunzmann S, Ottensmeier B, Speer CP, Fehrholz M. Effect of progesterone on Smad signaling and TGF-beta/Smad-regulated genes in lung epithelial cells. PLoS ONE. 2018;13:e0200661.
36. Sun Z, Ke L, Zhao Q, et al. The use of bioinformatics methods to identify the effects of SARS-CoV-2 and influenza viruses on the regulation of gene expression in patients. Front Immunol. 2023;14:1098688.
37. Villamayor L, Rivero V, Lopez-Garcia D, et al. Interferon alpha inducible protein 6 is a negative regulator of innate immune responses by modulating RIG-I activation. Front Immunol. 2023;14:1105309.
38. Assou S, Ahmed E, Morichon L et al. The Transcriptome Landscape of the In Vitro Human Airway Epithelium Response to SARS-CoV-2. Int J Mol Sci 2023;24.
39. Nakamura M, Kamiya K, Furuhata A, Ikeda K, Niyonsaba F. S100A7 Co-localization and Up-regulation of Filaggrin in Human Sinonasal Epithelial Cells. Curr Med Sci. 2021;41:863–8.
40. Miwa M, Hasan S, Miwa M, Okubo K. Filaggrin exists in human nose. Allergol Int. 2016;65:338–40.
41. Gao W, Gong J, Mu M, et al. The Pathogenesis of Eosinophilic Asthma: A Positive Feedback Mechanism That Promotes Th2 Immune Response via Filaggrin Deficiency. Front Immunol. 2021;12:672312.
42. Palmer CN, Ismail T, Lee SP, et al. Filaggrin null mutations are associated with increased asthma severity in children and young adults. J Allergy Clin Immunol. 2007;120:64–8.
43. Lee KH, Cho KA, Kim JY, et al. Filaggrin knockdown and Toll-like receptor 3 (TLR3) stimulation enhanced the production of thymic stromal lymphopoietin (TSLP) from epidermal layers. Exp Dermatol. 2011;20:149–51.
44. Bao K, Yuan W, Zhou Y, et al. A Chinese Prescription Yu-Ping-Feng-San Administered in Remission Restores Bronchial Epithelial Barrier to Inhibit House Dust Mite-Induced Asthma Recurrence. Front Pharmacol. 2019;10:1698.
45. Sherrill JD, Kc K, Wu D, et al. Desmoglein-1 regulates esophageal epithelial barrier function and immune responses in eosinophilic esophagitis. Mucosal Immunol. 2014;7:718–29.
46. Polivka L, Hadj-Rabia S, Bal E, et al. Epithelial barrier dysfunction in desmoglein-1 deficiency. J Allergy Clin Immunol. 2018;142:702–6. e7.

47. Qiao W, Xie T, Lu J, Jia T, Kaku K. Identification of potential hub genes associated with atopic dermatitis-like recombinant human epidermal model using integrated transcriptomic and proteomic analysis. Biomol Biomed. 2024;24:89–100.
48. Zhang Y, Black KE, Phung TN, et al. Human Airway Basal Cells Undergo Reversible Squamous Differentiation and Reshape Innate Immunity. Am J Respir Cell Mol Biol. 2023;68:664–78.
49. Jonsdottir HR, Arason AJ, Palsson R, et al. Basal cells of the human airways acquire mesenchymal traits in idiopathic pulmonary fibrosis and in culture. Lab Invest. 2015;95:1418–28.
50. Bankoti K, Wang W, Amonkar GM, et al. Airway Basal Stem Cells in COVID-19 Exhibit a Proinflammatory Signature and Impaired Mucocililary Differentiation. Am J Respir Cell Mol Biol. 2024;70:26–38.
51. Ruysseveldt E, Martens K, Steelant B. Airway Basal Cells, Protectors of Epithelial Walls in Health and Respiratory Diseases. Front Allergy. 2021;2:787128.

# Figures

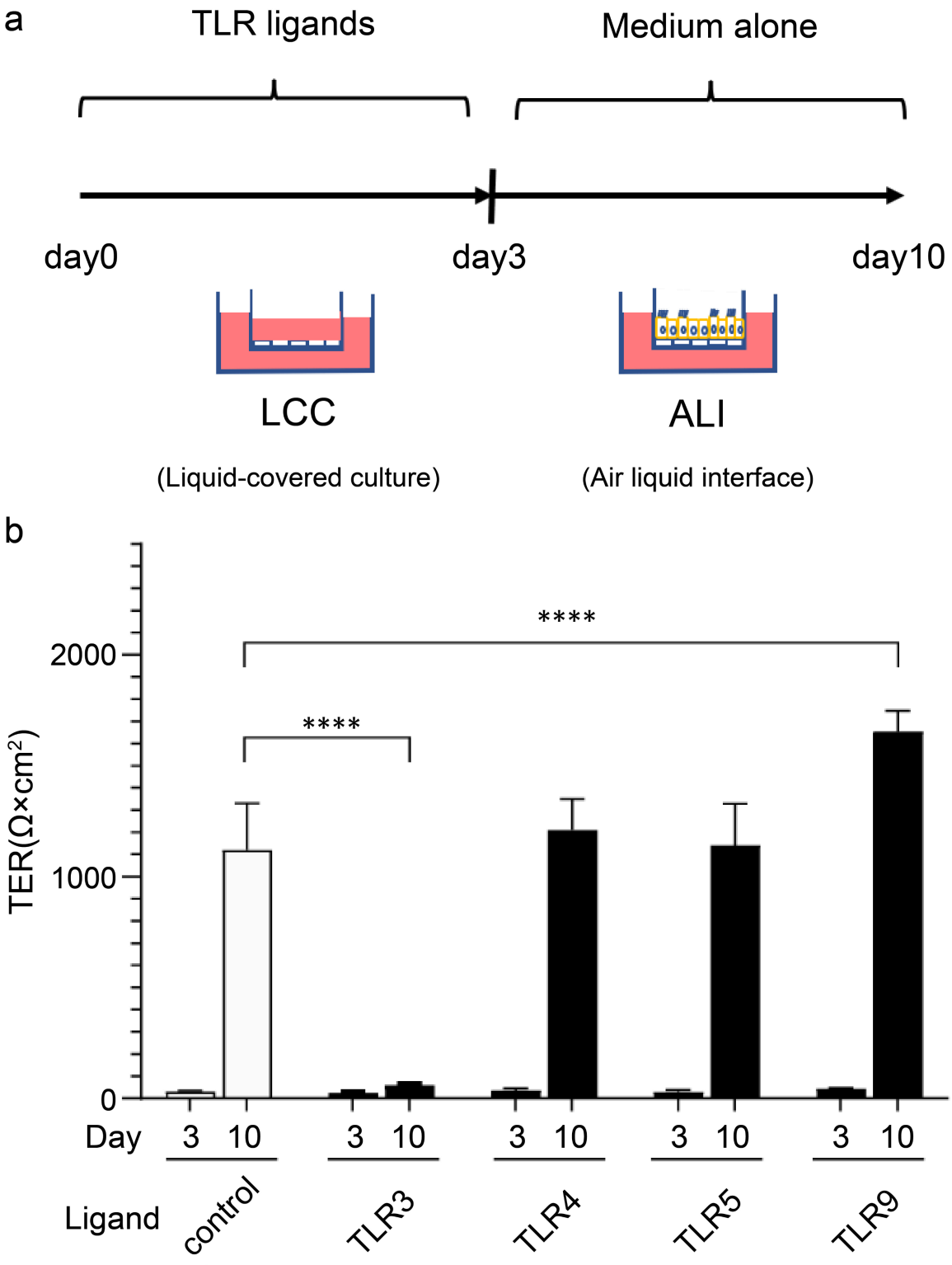
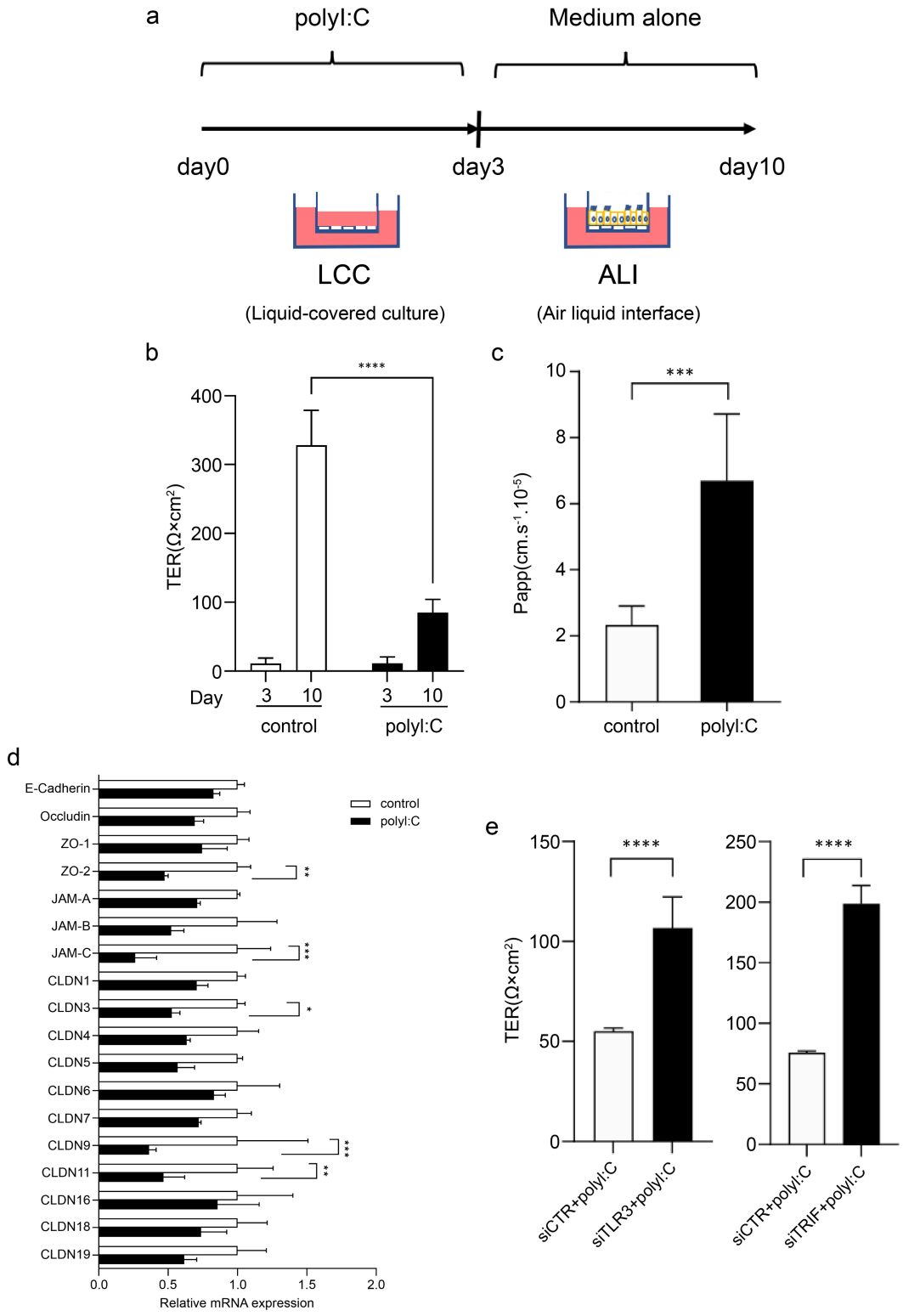



**Figure 1**

Effects of various TLR ligands on epithelial barrier function in NHBECs.

(a) Time course of experiment. (b) NHBECs were treated with or without ligands for TLR3, TLR4, TLR5, and TLR9 during the liquid-covered culture (LCC) phase, followed by ALI culture without further

stimulation. TEER was measured during the ALI phase, starting on day 3. Data are presented as mean ± SD (n = 4). ****p < 0.0001.

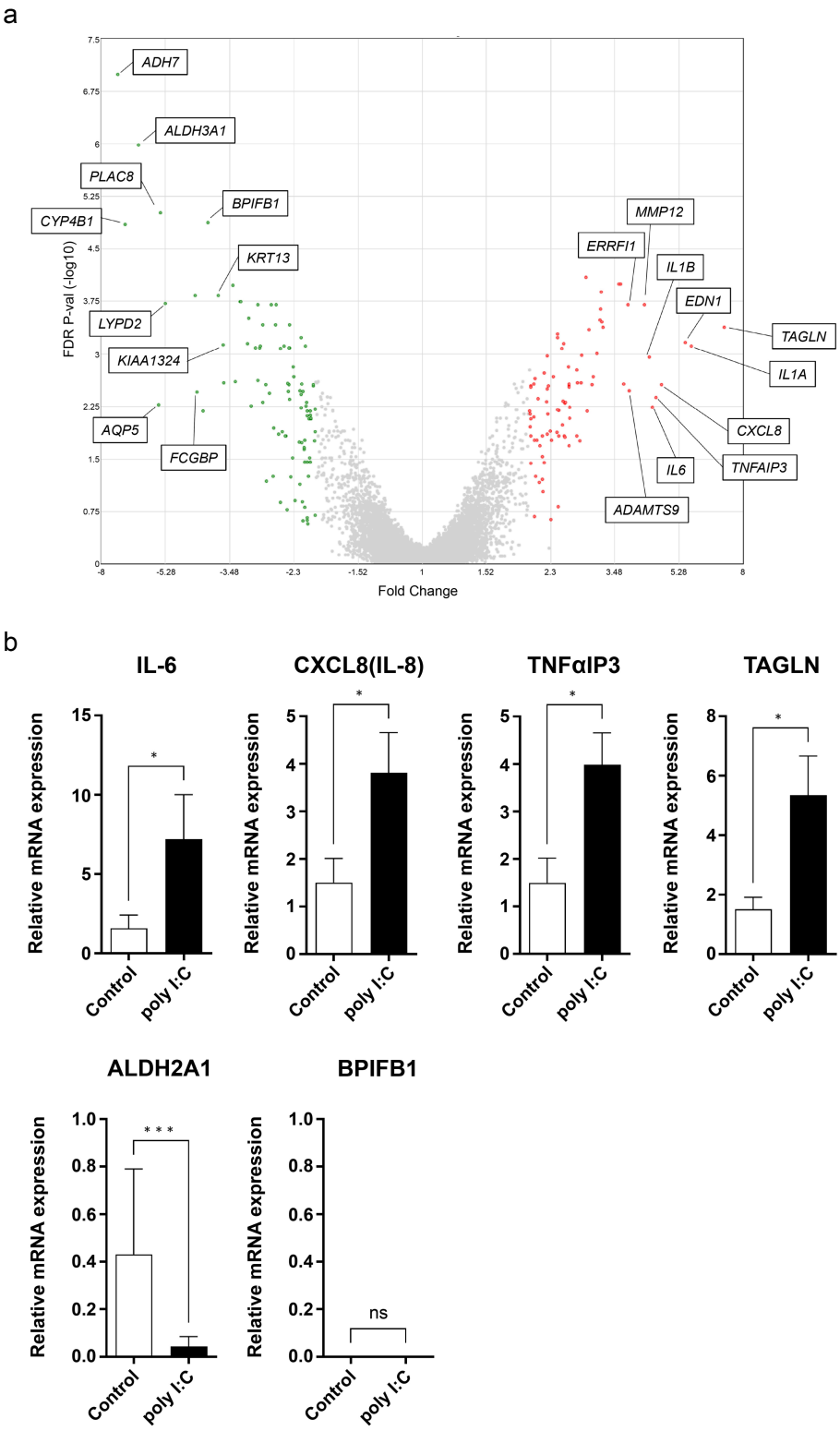



## Figure 2

Epithelial barrier dysfunction of VA10 by poly I:C treatment in LCC.

(a) Time course of experiment. (b) VA10 cells were treated with or without poly I:C during the liquid-covered culture (LCC) phase, followed by ALI culture without further stimulation. TEER was measured during the ALI phase, starting on day 3. Data are presented as mean ± SD (n = 9). ****p < 0.0001. (c) FITC-dextran permeability was measured on day 10. Results are expressed as mean ± SDs, n= 3; ***p < 0.001. (d) Confirmation of the mRNA expression of barrier related genes using real-time PCR on day 10. RT-qPCR analysis of E-cadherin, JAM-A, -B, and -C; Zo-1 and -2; and claudin-1, -3, -4, -5, -6, -7, -9, -11, -16, -18, and -19 mRNA expression. Results are expressed as the mean ± SD, n= 3; ***p < 0.001. (e) Confirmation of epithelial barrier dysfunction via the TLR3/TRIF pathway in VA10 cells.

VA10 cells were transfected with control siRNA, siTLR3, or siTRIF for 24 h, added to a Transwell plate, and cultured with or without poly I:C in LCC. TEER measurements were initiated at the start of the ALI culture (day 3), and the results obtained on day 10 are presented. Comparison with poly I:C treatment is shown (left: siCTR+poly I:C vs. siTLR3+poly I:C; Right: siCTR+poly I:C vs. siTRIF +poly I:C). Results are expressed as mean ± SDs, n = 3; ****p < 0.0001.




## Figure 3

PolyI:C-induced gene alterations in basal cells and following differentiation (day 10).

(a) Total RNA was extracted from NHBECs on day 10 in the poly I:C-stimulated and non-stimulated LCC groups, and gene analysis was performed using DNA microarrays. Figure A presents a volcano plot showing differentially expressed genes on day 10. The x-axis represents the signed fold change plotted

on a $\log_2$ scale, and the y-axis represents the $-\log_{10}$ (FDR). Green and red dots indicate significantly downregulated (FDR < 0.05, fold change ≤ -2.0) and upregulated (FDR < 0.05, fold change ≥ 2.0) genes, respectively. (b) Verification of gene expressions**.** Gene analysis was performed using DNA microarrays. The microarray results were used to select genes at the top and bottom of the expression rankings, and their expression levels were confirmed via real-time PCR.

Real-time PCR was performed to confirm the expression levels of TAGLN, TNFAIP3, IL-6, IL-8, ALDH3A1, and BPIFB1. Results are summarized as mean ± SDs, n=4, *p < 0.05, ***p < 0.001. The gene expression levels of all PCR samples were normalized to those of glyceraldehyde-3-phosphate dehydrogenase (GAPDH), a housekeeping gene.

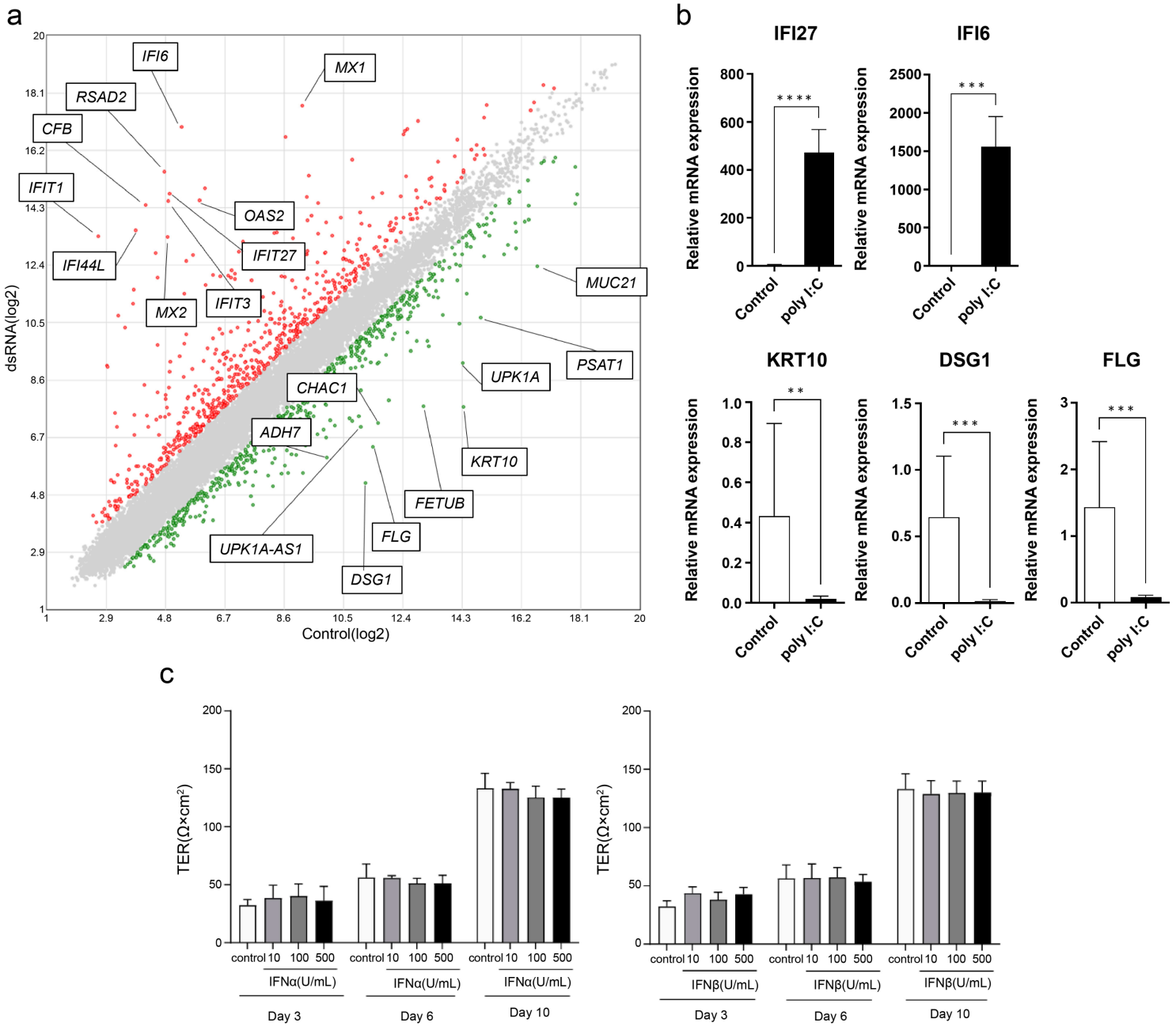



**Figure 4**

PolyI:C-induced gene alterations in basal cells and following differentiation (day 3).

(a) Total RNA was extracted from NHBECs on day 3 in the poly I:C-stimulated and non-stimulated LCC groups, and gene analysis was performed using DNA microarrays. Figure A presents scatter plots of gene expression on day 3: green, downregulated genes; red, upregulated genes. Day 3 data represent a single pooled sample derived from three independent cultures (n = 1)**.** (b) Verification of gene expressions. Gene analysis was performed using DNA microarrays. The microarray results were used to select genes at the top and bottom of the expression rankings, and their expression levels were confirmed via real-time PCR. Real-time PCR was used to confirm the expressions of IFI27, IFI6, FLG, KRT10, DSG1. Results are mean ± SDs, n=8, *p < 0.05, **p < 0.01, ***p < 0.001.

The gene expression levels of all PCR samples were normalized to those of glyceraldehyde-3-phosphate dehydrogenase (GAPDH), a housekeeping gene.

(c) Effects of type I IFN treatment of VA10 cells on airway epithelial barrier function. IFN stimulation of VA10 in LCC was performed as described previously for poly I:C treatment. TEER was measured in IFNα-stimulated (left) and IFNβ-stimulated (right) groups in ALI culture. Results are expressed as the mean ±SDs, n=6.

## Supplementary Files

This is a list of supplementary files associated with this preprint. Click to download.

- OkamotoSupplements.docx